

*Mass Profiles and Shapes of Cosmological Structures*  
*G. Mamon, F. Combes, C. Deffayet, B. Fort (eds)*  
*EAS Publications Series, Vol. ?, 2005*

## CAUSTICS IN DARK MATTER HALOES

Roya Mohayaee<sup>1</sup>, Stephane Colombi<sup>1</sup>, Bernard Fort<sup>1</sup>, Raphael Gavazzi<sup>2</sup>,  
 Sergei Shandarin<sup>3</sup> and Jihad Touma<sup>4</sup>

**Abstract.** Caustics are formally singular structures that frequently form in collisionless media. The non-negligible velocity dispersion of dark matter particles renders their density finite. We evaluated the maximum density of the caustics within the framework of secondary infall model of formation of dark matter haloes. The result is then used to demonstrate that caustics can be probed by properly stacking the weak-lensing signal of about 600 haloes. CFHTLS accompanied by X-ray observations and the space-based experiments like SNAP or DUNE can provide us with the required statistics. The extension of our results to more realistic models including the effects of mergers is outlined.

### 1 Introduction

Under the gravitational instability, cold streams of dark matter with different velocities cross at *caustic* surfaces. The density of dark matter at caustics formally diverges and in the regions bounded by caustics the velocity field is multi-valued. The full description of the evolution of the fluid is provided by the Vlassov-Poisson equation, in 6-dimensional phase space. Direct numerical integration of this equation remains a challenging task and so far is best achieved for systems with low number of dimensions and or with strong symmetry constraints (see *e.g.* Alard & Colombi 2004 and references therein). The most popular alternative to the full integration of this equation is to sample the phase space with discrete particles. However, extremely large number of particles is needed to sample the fine-structure of the phase space and significant softening of the forces is required to avoid spurious collisional effects which would smear out the caustics (see *e.g.* Binney 2004, Melott et al. 1997).

<sup>1</sup> IAP, Institut d'Astrophysique de Paris, 98 bis bd Arago, Paris, France

<sup>2</sup> Laboratoire d'Astrophysique, OMP, 14 Av Edouard Belin, F-31400 Toulouse, France

<sup>3</sup> Department of Physics and Astronomy, University of Kansas, KS 66045, U.S.A.

<sup>4</sup> Department of Physics, Center for Advanced Mathematical Sciences, American University of Beirut, Beirut, Lebanon

Until a full 3-dimensional solution of Vlassov-Poisson equation or ground-breaking resolution in N-body simulations or other innovative solutions are achieved, (semi-)analytic modeling of haloes can provide approximative description of the dynamics at fine scales.

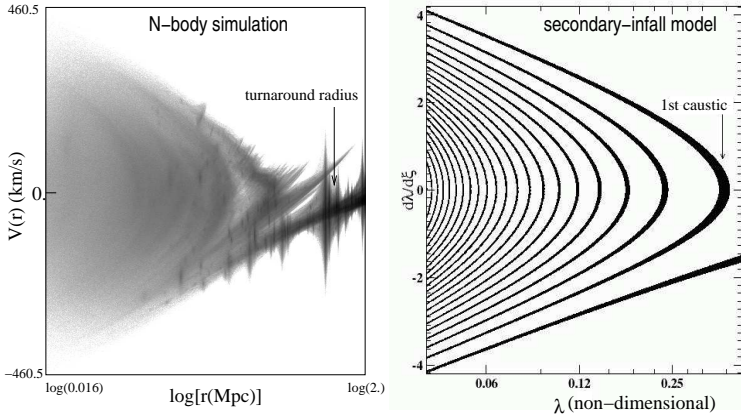


**Fig. 1.** *Left panel:* Phase space diagram (radial velocity versus radius) of a Milky-Way-type halo, taken from a PM simulation with 16 millions of particles on a 1024 grid in a 4 Mpc simulation box realized at IDRIS computing center (CNRS). The halo has about 8 million particles in its virial radius and contains only 40 substructures, as they are rapidly disrupted due to softening of the forces in the PM routine. The smoothness of the gravitational potential (there are many particles per softening length) enables us to see the caustics since the phase-space structure can survive the relaxation effects. *Right panel:* Secondary infall model's prediction of the phase space of a spherical halo in smooth accretion. The caustics in the model are far better resolved as compared to the left panel, due to the simple assumption of sphericity, no abrupt major merger and no substructures. The panel clearly shows that the streams *cool down* as they collapse: a consequence of phase-space volume conservation as filamentation builds up.

Analytic works on the halo density profile, and its caustics, started with the works of Gott (1975) and Gunn (1977). In an Einstein-de Sitter Universe a spherical over-density expands and then turns around to collapse. After collapse and at late times, the fluid motion becomes selfsimilar: its form remains unchanged when length are re-scaled in terms of the radius of the shell which is currently turning around ( $r_{\text{ta}}$ ) and falling onto the galaxy. Self-similar solutions give power-law density profiles which is convolved with many small-scale spikes *i.e.* caustics (Fillmore and Goldreich 1984, Bertschinger 1985a, 1985b).

In the self-similar accretion model, Newton's law is reformulated as

$$\frac{d^2\lambda}{d\xi^2} + \frac{7}{9} \frac{d\lambda}{d\xi} - \frac{8}{81} \lambda = -\frac{2}{9\lambda^2} M(\lambda), \quad (1.1)$$

by using the non-dimensional variables

$$\lambda = \frac{r(t)}{r_{\text{ta}}(t)} \quad ; \quad \xi = \ln \left( \frac{t}{t_{\text{ta}}} \right) \quad ; \quad M(\lambda) = \frac{3}{4\pi} \frac{m(r,t)}{\rho_H r_{\text{ta}}^3},$$

where  $m(r,t)$  is the mass inside a radius  $r$  [ $m(r,t)$  is not constant due to shell-crossing],  $\rho_H = 1/6\pi G t^2$  and  $t_{\text{ta}}$  is the turnaround time for a given particle (*i.e.* when the particle is at its largest radius). This reformulation also assumes the power-law initial condition

$$\frac{\delta M_i}{M_i} = \left( \frac{M_i}{M_0} \right)^{-\epsilon} \quad (1.2)$$

where  $M_0$  is some reference mass and  $M_i$  is the unperturbed mass within the initial radius  $r_i$ . It might appear that the asymptotic self-similarity is a direct outcome of the power-law initial mass profile. However, it has been shown that starting from a generic initial condition, a power-law density profile is achieved prior to the first turnaround time (Moutarde et al 1991). The turnaround radius increases with time as  $r_{\text{ta}} \approx t^{(2/3)(1+1/3\epsilon)}$  and hence the mass inside the turnaround radius increases as  $M_{\text{ta}} \approx (1+z)^{-1/\epsilon}$ . This scaling compares with that of the characteristic mass in a scale-free hierarchical clustering Universe  $M_* \approx (1+z)^{-6/(n+3)}$  where the power-spectrum of initial density fluctuations is  $P(k) \approx k^n$ . A central point mass perturbation corresponds to  $\epsilon = 1$ ,  $r_{\text{ta}} \approx t^{8/9}$ ;  $M_{\text{ta}} \approx 1/(1+z)$  which is the only case considered here. Extension of our results to more realistic initial conditions (*e.g.*  $\epsilon \sim 0.2$ ) will follow in forthcoming works.

For a perfectly cold dark matter medium, the density profile close to the  $k$ th caustic at  $\lambda_k$  is (Bertschinger 85b)

$$\frac{\rho_0(\lambda)}{\rho_H} = \left( \frac{\pi^2}{4\sqrt{-2\lambda_k''}} \frac{e^{-2\xi_k/3}}{\lambda_k^2} \right) \frac{1}{\sqrt{\lambda_k - \lambda}}; \quad \sigma = 0. \quad (1.3)$$

(The values of the various quantities  $\xi_k$ ,  $\lambda_k$ ,  $\lambda_k''$  are given in Bertschinger 1985b.)

When the temperature of particles is not strictly zero, caustic positions are shifted by a small value  $\delta\lambda$  and the density near the caustic is modified as:  $\rho_\sigma(\lambda) = \int dv \rho_0 [\lambda - \delta\lambda(v)] f(v)$ . A simple top-hat velocity distribution function,  $f(v)$ , yields

$$\frac{\rho_\sigma(\lambda)}{\rho_H} = \left( \frac{\pi^2}{4\sqrt{-2\lambda_k''}} \frac{e^{-2\xi_k/3}}{\Delta_k \lambda_k^2} \right) \begin{cases} \sqrt{\lambda_k^+ - \lambda} - \sqrt{\lambda_k^- - \lambda} & \text{for } \lambda < \lambda_k^-, \\ \sqrt{\lambda_k^+ - \lambda} & \text{for } \lambda_k^- < \lambda < \lambda_k^+, \\ 0 & \text{for } \lambda > \lambda_k^+, \end{cases} \quad (1.4)$$

for the density near the  $k$ -th caustic, where  $\lambda_k^- = \lambda_k - \Delta_k$  and  $\lambda_k^+ = \lambda_k + \Delta_k$  and the thickness of the  $k$ -th caustic is  $\Delta_k$ . A simple re-scaling demonstrates that these densities are universal: they are valid for all caustics and irrespective of size and mass of their halo. (for full details see Mohayaee & Shandarin 2005).

Caustics could have immediate impact for dark matter search experiments. Their high density and the fact that they stay well-separated from each other (see

left panel of Fig 2) can leave detectable fluctuations in the annihilation products of the dark matter particles [if it constitutes for example of self-annihilating axions or neutralinos] (see *e.g.* Sikivie & Ipser 1992, Sikivie et al. 1997) and or in the weak lensing data, which we shall study here (see *i.e.* Hogan 2001, Charmosis 2003, Gavazzi et al. 2005).

For weak lensing, the Abel integral relates the 3-dimensional density ( $\rho$ ) and the 2-dimensional density profiles ( $\Sigma$ ) by (see Gavazzi et al. 2005 and references therein for full details)

$$\Sigma(\lambda) = 2r_{ta} \int_{\lambda}^{\infty} \frac{\rho(\lambda')\lambda' d\lambda'}{\sqrt{\lambda'^2 - \lambda^2}}. \quad (1.5)$$

We numerically integrate the above expression, for the density profiles (1.3) and (1.4). We define a pseudo-shear:  $\Gamma(\lambda) = (\bar{\Sigma} - \Sigma)/\rho_H r_{ta}$  and the corresponding noise level  $\Gamma_N$ . For an EdS cosmology, and considering an annulus of inner and outer radii  $\lambda_1$  and  $\lambda_2$  respectively, it is straightforward to write  $\Gamma_N$  in the following units:

$$\Gamma_N(\lambda_1, \lambda_2) = 2.16 \frac{D_{os}}{D_{ls}} \left( \frac{5 \text{Mpc}}{r_{ta}} \right)^2 (1 + z_l)^3 \times \sqrt{\frac{30 \text{ arcmin}^{-2}}{n}} \left( \frac{\sigma_e}{0.3} \right) \frac{1}{\sqrt{\lambda_2^2 - \lambda_1^2}}. \quad (1.6)$$

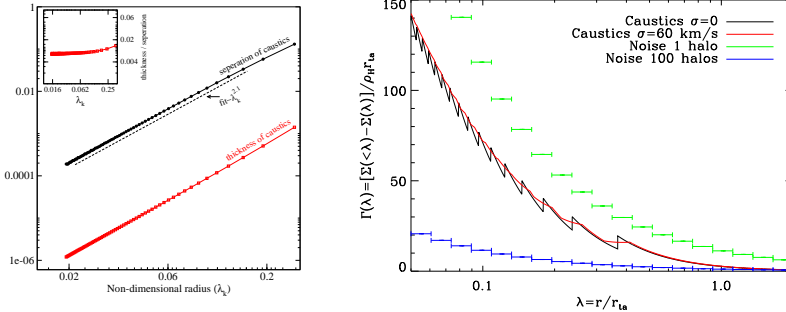


**Fig. 2.** *Left panel Left panel ; Main plot:* The top line (filled circles) shows the separation of caustics,  $\lambda_k - \lambda_{k+1}$ , as a function of the distance,  $\lambda_k$ , from the center. The bottom line shows the thickness of the caustics. *Left panel ; Inset:* The ratio of the thicknesses of the caustics to their separations,  $2\delta\lambda_k/(\lambda_k - \lambda_{k+1})$ , is shown as a function of their radii. This panel demonstrates that in the course of the gravitational evolution streams remain well-isolated from each other in spite of the fact that their separations diminish. *Right Panel:* Pseudo-shear is plotted for two values of  $\sigma$ : cold medium  $\sigma = 0$  (black curve) and warm medium  $\sigma \sim 60$  km/s (red curve). Unphysically large value of velocity dispersion is therefore required to smear out the caustics. The green (resp. blue) binned curve is the noise level for one (resp. 100 stacked) halo(es).

Fig. 2 shows pseudo-shear as a function of distance from the center of the cluster for the thermal velocity dispersions  $\sigma = 0$  km/s and  $\sigma = 60$  km/s. Comparing

these curves, one can see that the sawtooth patterns due to caustics survive significantly high temperatures. Next, we consider the noise level for a fiducial halo at redshift  $z_l = 0.3$  [since intermediate redshift haloes at  $z_l \sim 0.2 - 0.5$  are the most likely targets; see Gavazzi et al. 2005 for further details]. and a turnaround radius  $r_{ta} = 5\text{Mpc}$  which is a typical value for clusters (upper green binned curve). With a single halo the detection of caustics is impossible. Since, the noise falls with the square-root of the number of lenses (as well as the source), if one could stack the signal from a few tens of clusters, the noise level will be low enough to be sensitive to caustics as a whole (lower blue curve). Systematic error can arise due to the intrinsic ellipticity of the clusters. The precise effect of which can be well-studied with the help of N-body simulations in future works. However, due to its significant separation from the second caustic and the turnaround radius, it is likely that the first outer caustic would survive smearing due to substructures and ellipticity of the haloes.

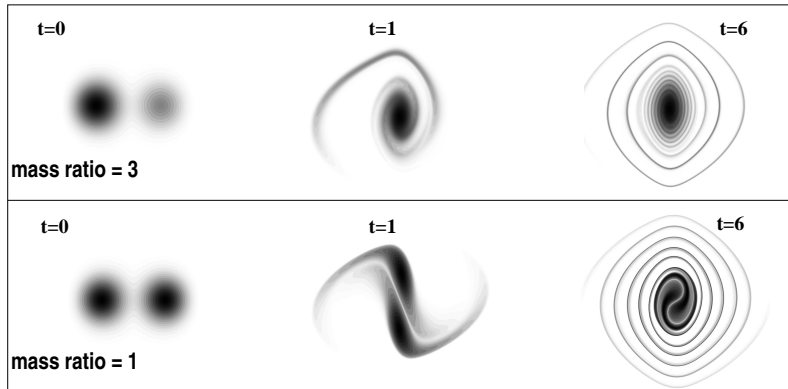


**Fig. 3.** Phase space of a 1D-1D simulation of merger of two haloes using the waterbag code of Colombi and Touma (2005). The simulation indicates that in the merger of two haloes, phase-space folds do not mix and the topology of caustics remains intact.

Although in this work we have considered dynamics of a simple isolated haloes, we believe that the results can be extended to haloes growing in cosmological environment. One of the short-comings of the secondary infall model could be that it ignore the hierarchical scenario of merger. Merger might lead to distorted topology for the caustics and hence render them practically non-detectable. However, minor mergers which are on average isotropic are well-described by the self-similar model, which assumes a spherically symmetric accretion. Thus such mergers would not erase the caustics. Indeed even if the condition of isotropy is not satisfied, the caustics retain their shapes quite well. The numerical solution to a 1-dimensional Vlassov-Poisson equation clearly suggests this fact in Fig. 3. In mergers of unequal mass haloes the smaller halo wraps around the larger halo without disrupting its phase-space structure. In fact it populates it in a coherent manner as shown in the top panel of Fig. 3.

In a major merger, a similar situation follows. The phase sheets of the two caustics do not mix, However, they fold closely together in phase space [bottom row of Fig. 3]. Thus, Fig 3 demonstrates that in the merger of two haloes the topology of caustics remains intact.

Another important feature demonstrated well in Fig. 3 is the gravitational cooling effect. With the increase of dynamical time ( $t$ ) the coarse-grain velocity dispersion which is related to the number of folds in the phase space increases. However, each fold cools down and becomes thinner, a surprising feature of a system with negative specific heat, but which can be understood roughly by the conservation of phase-space volume.

For a perfectly cold dark matter with zero velocity dispersion, caustics are singular objects with zero thickness and infinite density which form inevitably in the course of gravitational collapse. The small velocity dispersion of dark matter particles renders the density and the thickness of the caustics finite. The latter quantities, if observed, could provide direct evidence for the existence of dark matter and put bounds on its mass.

We have shown that the existence of dark matter caustics could be probed by properly stacking the weak lensing signal of a reasonable number of haloes. The main observational limitation is perhaps the precise estimation of the turnaround radius,  $r_{ta}$ , of superimposed haloes. However, the loss of a few percents relative accuracy in the determination of  $r_{ta}$  (or asphericity) can be compensated for by stacking about 600 haloes. Wide field surveys such as the ongoing CFHTLS accompanied by X-ray observations can provide the required statistics for a successful detection of caustics. The number of haloes required to be superimposed will be lowered by a further factor of 3 for future space-based experiments like SNAP or DUNE.

## References

Alard, C. & Colombi, S. 2005, MNRAS, 359, 123  
 Bertschinger, E., 1985a, ApJ, 58, 1  
 Bertschinger, E., 1985b, ApJ, 58, 39  
 Charbonneau, C., Onemli, V., Qiu, Z., & Sikivie, P. 2003, PRD, 67, 103502  
 Colombi, S. & Touma 2005, in preparation  
 Fillmore J.A. & Goldreich P. 1984, ApJ, 281, 1  
 Gavazzi, R., Mohayaee, R. & Fort, B. 2005, astro-ph/0506061, A& A in press  
 Gott, J.R., 1975, ApJ, 201, 296  
 Gunn, J.E., 1977 ApJ, 218, 592  
 Hogan, C., 2001 Phys. Rev. D, 64, 063515  
 Melott, A.L., Shandarin S.F., Splinter R.J. & Suto Y. 1997, ApJL, 479, 79  
 Mohayaee, R. & Shandarin, S. F. 2005, astro-ph/0503163, MNRAS in press.  
 Moutarde, F., Alimi, J.-M., Bouchet, F. R., Pellat, R. & Ramani, A. 1991, ApJ, 382, 377  
 Sikivie, P., & Ipser, J. 1992, Phys. Lett. B, 291, 288  
 Sikivie, P., & Tkachev, I.I., Wang Y. 1997, Phys. Rev. D, 56, 1863